Supporting Information for:

Spatiotemporal Control of Calcium Carbonate Nucleation Using Mechanical Deformations of Elastic Surfaces

Jay Taylor, Abhiteja Konda, and Stephen A. Morin*

Dept. of Chemistry, University of Nebraska-Lincoln, Hamilton Hall, Lincoln, NE 68588.
and
Nebraska Center for Materials and Nanoscience, University of Nebraska-Lincoln, Lincoln, NE 68588.

* To whom correspondence should be addressed. Telephone: (402) 472-4608. Fax: (402) 472-9402. E-mail: smorin2@unl.edu.

Materials and Methods

Materials 1.1.

The surfaces and reactors were made from PDMS, Sylgard® 184 silicone elastomer kit (Dow Corning, Midland, MI), made in a 10:1 base to curing agent ratio. The fluidic reactors also consisted of the softer silicone Ecoflex® (00-30) (Smooth-On, Inc.), which was prepared by mixing equal part A and part B. $CaCO_3$ growth solutions were made using $Na_2CO_3 \cdot H_2O$ (CAS 5968-11-6) and $CaCl_2 \cdot 2H_2O$ (CAS 10035-04-8), purchased from Sigma-Aldrich, St. Louis, MO and used as received. Phosphate Buffer was made from Na_2HPO_4 (CAS 7558-79-4) and NaH_2PO_4 (7558-80-7), purchased from Fisher Scientific and used as received. The pH for the solutions were adjusted using dilute solutions of NaOH (CAS 1310-73-2) and HCl (CAS 7647-01-0), purchased from Fisher Scientific and used as received.

1.2 Methods

1.2.1. PDMS Film Fabrication. PDMS prepolymer was poured onto the polished side of a 6” silicon wafer, spread to a thickness of 500 μm using an applicator (Zehnter testing instruments ZUA 200), and placed into a 60°C oven for 60 minutes and used within 24 hours of curing.

1.2.2. Oxidized PDMS Fabrication. The above films were either used as prepared or were oxidized in an oxygen plasma chamber (Plasma Etch Inc., Carson City, NV, Model# PE-25 Series) at a FWD bias of 15 W for 10 seconds, then placed into a 50 mL centrifuge tube with an aqueous buffer solution consisting of 1.0 M sodium phosphate set to pH 7.00, and placed into a 80°C oven for 60 minutes to slowly etch away the brittle surface layer restoring its elastic properties.[S1] The substrates were then removed and rinsed with DI water and dried under a stream of N_2 gas.

1.2.3. Measurements of Surface Free Energy. The surface energy of the native and oxidized PDMS samples were performed using an established method by Owens, Wendt, Rabel, and Kaelble (OWRK).[S2-S4] Static contact angle measurements were taken with three test liquids:

Nanopure 18.2 MΩ water, glycerol, and ethylene glycol. " Three replicate droplets were made on native and oxidize films at five different strain values (ε = 0.00, 0.25, 0.50, 0.75, 1.00) for each test liquid. The contact angle was recorded after 20 seconds of being placed on the PDMS surface and the experiment was repeated on two additional and identical surfaces (N = 3). The mean contact angle θ was plotted against the ratio of the squares of the polar ($\gamma_L{}^p$) and dispersive ($\gamma_L{}^d$) components of their respective surface tensions according to the following equation:

$$\frac{\gamma_L(\cos\theta+1)}{2\sqrt{\gamma_L^d}} = \sqrt{\gamma_s^p}\left(\frac{\sqrt{\gamma_L^p}}{\sqrt{\gamma_L^d}}\right) + \sqrt{\gamma_S^d} \qquad \text{Eq.S1}$$

where,

$$\gamma_L = \gamma_L^p + \gamma_L^d \qquad \text{Eq. S2}$$

$\gamma_S{}^p$ and $\gamma_S{}^d$ represent the polar and dispersive components of the substrate found though the linear regression analysis of Eq. S1 (Fig. S1 and Table S1 and Table S2).

For the three test liquids, we used reported values of the polar and dispersive components of their surface tensions (Table S3) and inserted these values into Eq. S1 along with the averaged measured contact angle for each test liquid (Figure S1). We then fit this data to an equation for a straight line (y = mx + b), so that the square of the slope and the square of the extrapolated y-intercept were used for the polar and dispersive components of the measured surface energy.

The use of static contact angles is standard practice when applying the OWRK method. This choice, over dynamic contact angle measurement techniques, was not expected to impact our primary conclusions as it was changes in surface energy that was most important in this study.

1.2.4. Fabrication of $CaCO_3$ Fluidic reactor. A milli-fluidic channel was designed in Autodesk Inventor and printed on a Stratasys ABS 3D printer. The features of the part were exposed to acetone vapor to smooth the surface texture. Then a layer of Exoflex-0030 is poured across the base of the mold, placed into an 80°C oven for 10 minutes to cure, then PDMS is used to fill the rest of the mold and placed into an 80°C oven for 25 minutes. The reactor is peeled away from the mold, and inlets and outlets were created using a biopsy punch.[S5]

1.2.4. Measuring $CaCO_3$ growth rate on PDMS substrates. PDMS film is placed in a custom compression-based microfluidic set up (Fig. S2). For each experiment, we stretched the substrate to the appropriate strain value, and held it strained by compressing the reactor and film together using our apparatus (Fig. S2B,C). The device was placed under a horizontal axis microscope from Zeiss (Axio Scope.A1) equipped with a mechanical stage (Fig. S2A). Nanopure water was flowed through the device at a rate of 0.150 mL/min for 10 minutes before 5.00 mM solutions of $CaCl_2$ and Na_2CO_3 set to pH 10.80 were flown in at a rate of 0.050 mL/min (150 second resonance time in device). The supersaturation of $CaCO_3$ at these concentrations was calculated to be 5.25 using the MINTEQ2A software. We then collected a series of images tracking the formation of $CaCO_3$ nuclei under the microscope. Every 120 seconds a 11.25 mm^2 area was scanned for a total of 2400 seconds, and we tracked the number of crystals observed as a function of time. The images were exported into imageJ, underwent a color threshold and each picture was analyzed for particle size and location (Fig. S2D-G). It was assumed every nuclei that formed developed into a crystal of measurable size. The rate was extracted by measuring the slope of the crystal count verses time measured from the series of images.

We note that we settled on a pH of 10.8 to help control the speciation of the coupled equilibria in the precursor solutions. At a pH above the pKa of the carbonate ion (10.3), the dibasic form (CO_3^{2-}) is favored and nucleation is dominated by the very low K_{sp} of $CaCO_3$.

1.2.5 Subsequent Mineralization experiments. The successive mineralization experiments were performed by first measuring the nucleation rate of an oxidized film at a strain of ε = 0.00 using the procedure described in the previous section. We stopped the growth after 1200 seconds and flowed in nanopure water to gently rinse the surface and then stretched the surface to the designated strain value being sure to keep the films submerged in solution as tension was applied to remove drying effects from altering the nucleation behavior of this second growth step. We then performed the second mineralization experiment under the same conditions for 4800 seconds, while measuring the growth rate of $CaCO_3$.

1.2.6. Fabrication of micropatterned PDMS films. A CAD file was designed in Autodesk Inventor, exported to an SLA style 3D printer (Autodesk, Ember). The printed mold was exposed to 1H,1H,2H,2H,-perfluorooctyltrichlorosilane (CAS 78560-45-9) to render mold inert from reaction with PDMS. Next PDMS prepolymer was "doctor-bladed" across the chemically-treated mold, filling-in its micro-features. Then the mold was placed inside a vacuum chamber to remove any gas bubbles preventing the filling of the micro-features. Finally, the PDMS was placed in an 80 °C oven for 30 minutes. $CaCO_3$ was grown as described in previous sections, but the concentration was changed to 8.00 mM for both $CaCl_2$ solutions and Na_2CO_3 solutions and pH raised to 11.3 (to increase crystal density). Images were collected using confocal microscopy (Keyence laser scanning microscope VK-X200K Series).

1.2.7. FEA analysis of Molded PDMS. We performed finite element analysis (FEA) using ABAQUS to describe the deformation of the micropatterned PDMS films. In our model, we used reported hyperelastic material's constants (Table S4 and Table S5) to define the PDMS matrix.[S6] To simulate uniaxial tension, we applied a displacement equal to a ε = 1.00 pulling from each end of the film. We then applied wedged mesh of 0.100 mm and simulated its mechanical response showing plots of mechanical plane-strain (ε) experienced by the film.

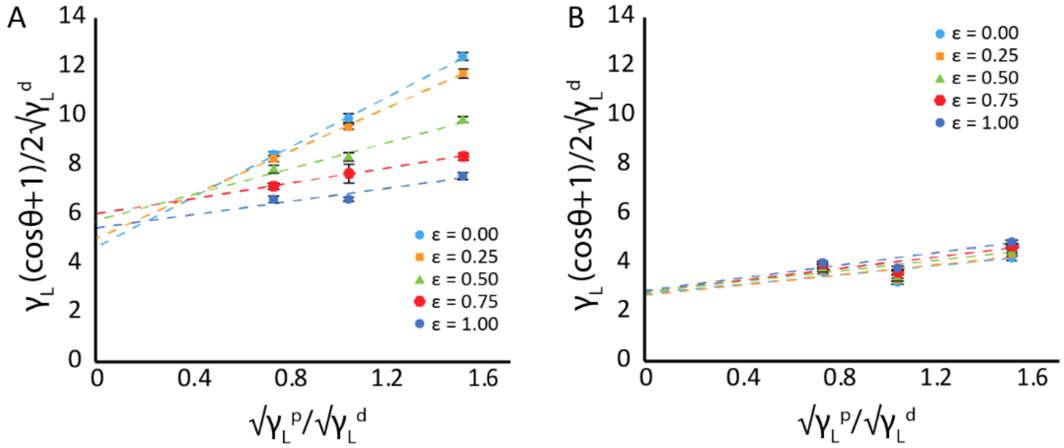

Figure S1: Plots to extrapolate the polar surface tension, $\gamma_S{}^p$, component and the dispersive surface tension component, $\gamma_S{}^d$, for the (A) oxidized film at 5 strain states and the (B) native film at the same 5 strain states following the OWRK (see above for more details).

Oxidized			
Strain (ΔL/L)	**γ_s (mJ/m^2)**	**γ_s^p (mJ/m^2)**	**γ_s^d (mJ/m^2)**
0.00	48.0	28.8	19.2
0.25	44.7	19.2	25.5
0.50	39.8	7.1	32.7
0.75	37.3	2.1	35.2
1.00	31.8	1.7	29.9

Table S1: Oxidized surface energy measurements obtained from analysis from Fig. S1.

Native Surface			
Strain (ΔL/L)	**γ_s (mJ/m^2)**	**γ_s^p (mJ/m^2)**	**γ_s^d (mJ/m^2)**
0.00	9.08	0.26	8.82
0.25	9.16	0.28	8.88
0.50	9.48	0.42	9.06
0.75	9.26	0.50	8.76
1.00	9.14	0.90	8.24

Table S2: Native surface energy measurements obtained from analysis from Fig. S1.

Surface Tension Components of Test Liquids			
Liquid	**γ_l (mJ/m^2)**	**γ_l^p (mJ/m^2)**	**γ_l^d (mJ/m^2)**
Water	72.8	51.0	21.8
Glycerol	63.4	33.4	30.0
Ethylene Glycol	48.0	17.1	30.9

Table S3: A list of the surface tension components used in the determination of surface free energy.[S2, S4]

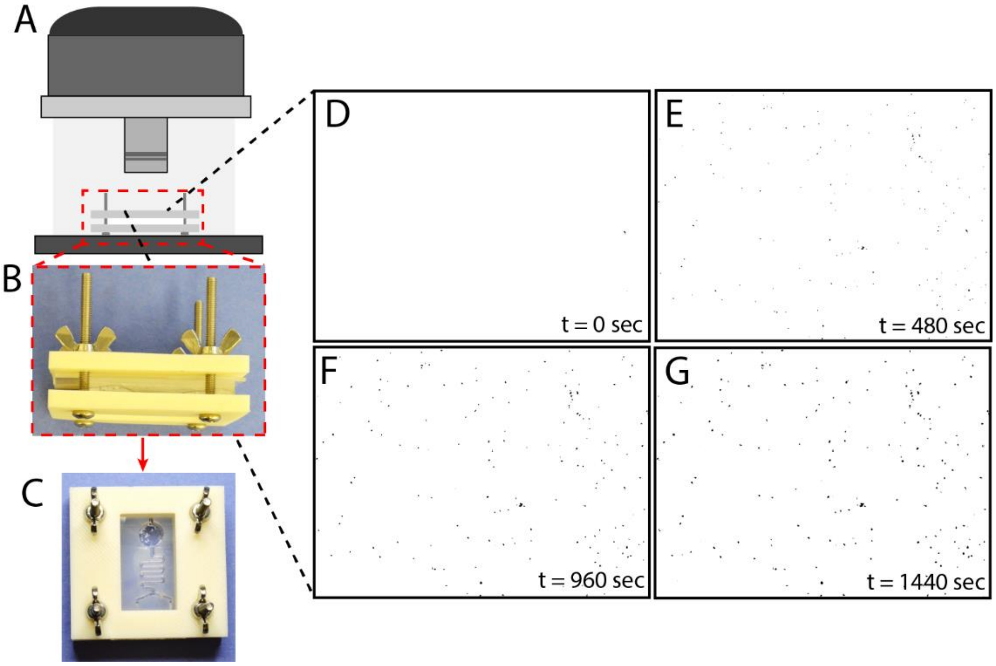

Figure S2: Experimental set-up for the growth of $CaCO_3$. A) Compression set-up is placed under a horizontal axis microscope. B) Optical image of the side view of compression apparatus and C) optical image of the top view of the compression set-up. D-E) Optical micrographs are captured every 120 seconds, exported to imageJ, where the nuclei' were counted and analyzed for size and location on the surface of the film.

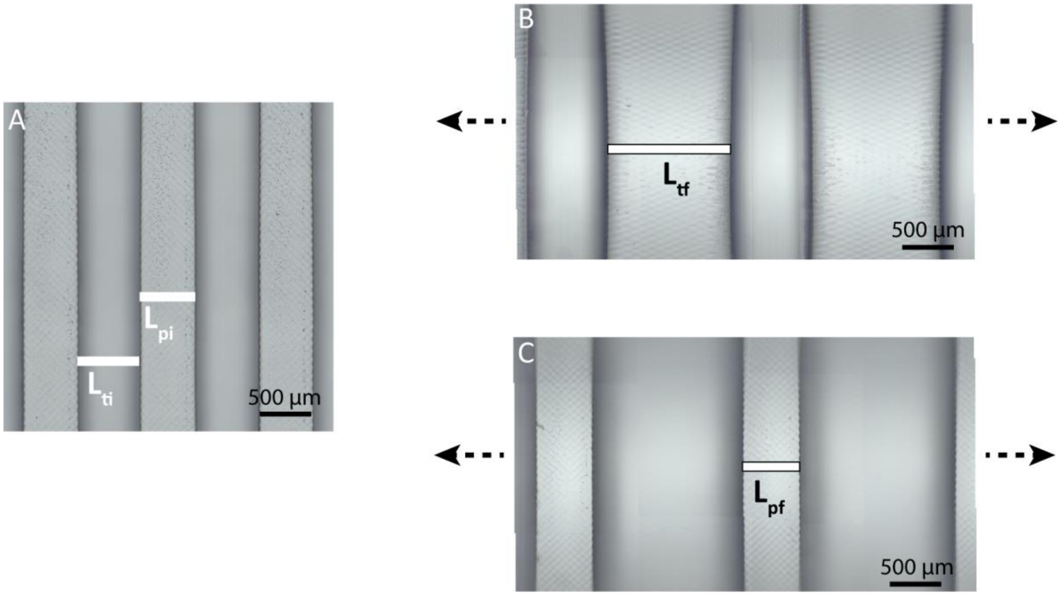

Figure S3: Optical microscope images of the deformation of the molded PDMS surface. A) An optical micrograph image of the molded PMDS at an applied strain, $\varepsilon = 0.00$, defining the initial peak length, L_{pi}, and the initial trough length, L_{ti}. B) An optical micrograph image focused on the bottom of the substrate at an applied $\varepsilon = 1.00$, defining the final trough length, L_{tf}, the strain in the trough was defined as $\varepsilon = (L_{tf} - L_{ti})/L_{ti}$. C) An optical micrograph image focused on the top of the peak, defining the final peak length, L_{pf}, the strain on the peak was defined as $\varepsilon = (L_{pf} - L_{pi})/L_{pi}$.

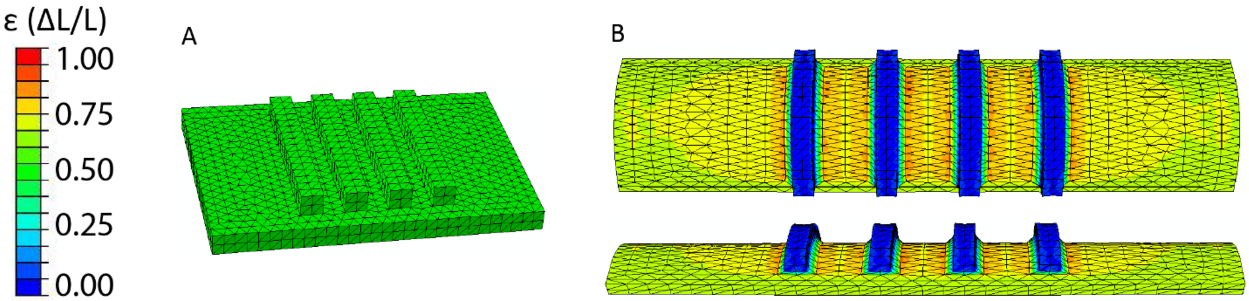

Figure S4: FEA of uniaxial tension of ε = 1.0 being applied to a molded PDMS films. A) image showing an undeformed molded PDMS structure. B) Top-down and side images depicting the deformation when a total displacement of 1.0 is applied to the substrate. Color bar shows in-plane strain.

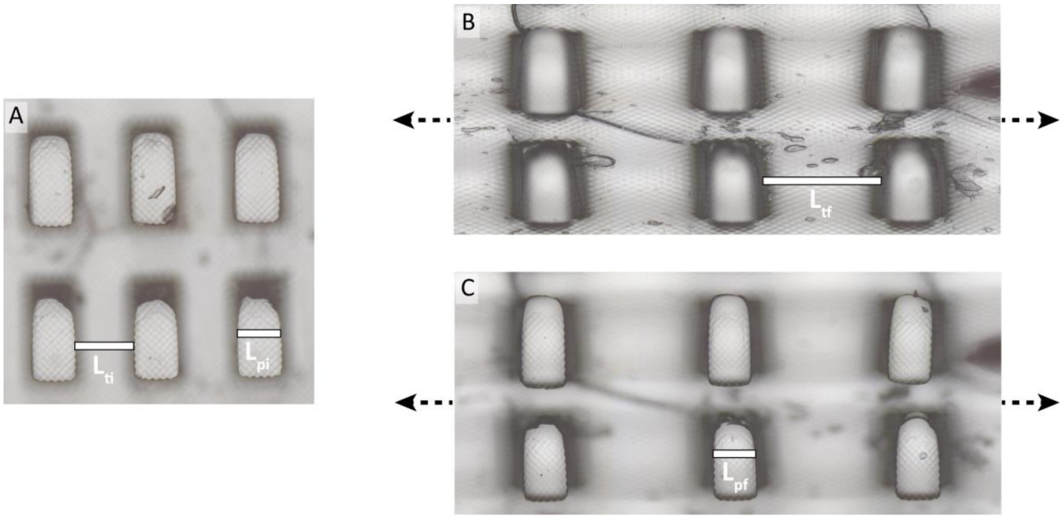

Figure S5: Optical microscope images of the deformation of the molded PDMS film's surface. A) An optical micrograph image of the molded PMDS at an applied $\varepsilon = 0.00$, defining the initial peak length, L_{pi}, and the initial trough length, L_{ti}. B) An optical micrograph image focused on the bottom of the substrate at an applied $\varepsilon = 1.00$, defining the final trough length, L_{tf}, the strain in the trough was defined as $\varepsilon = (L_{tf} – L_{ti})/L_{ti}$. C) An optical micrograph image focused on the top of the peak, defining the final peak length, L_{pf}, the strain on the peak was defined as $\varepsilon = (L_{pf} – L_{pi})/L_{pi}$.

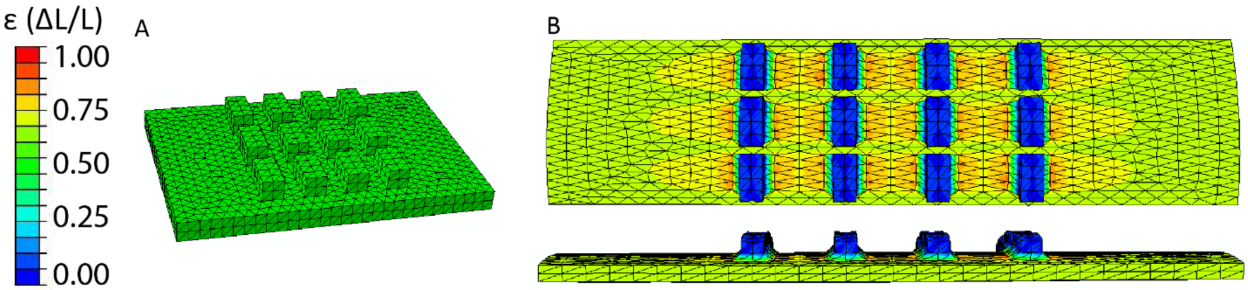

Figure S6: FEA of uniaxial tension of ε = 1.0 being applied to a molded PDMS films. A) image showing an undeformed molded PDMS structure. B) Top-down and side images depicting the deformation when a total displacement of 1.0 is applied to the substrate. Color bar shows in-plane strain.

Hyperelastic Materials Constants for PDMS

µ1 (MPa)	α1	µ2 (MPa)	α2	D1	D2
0.011426	0.131615	9.7991	3.6718	0	0

Table S4: Hyperelastic Materials Constants used in FEA analysis[S6]

Elastic Materials Constants for PDMS

Young's Modulus (MPa)	Poisson's Ratio
1.8	0.48

Table S5: Elastic Materials Constants used in FEA analysis[S6]

Supporting Information References:

S1. Bowen, J. J.; Taylor, J. M.; Jurich, C. P.; Morin, S. A., *Adv. Funct. Mater*. 2015, ***25***, 5520-5528.

S2. Giuffre, A. J.; Hamm, L. M.; Han, N.; De Yoreo, J. J.; Dove, P. M., *Proc. Natl. Acad. Sci. USA*, 2013, **110**, 9261-9266.

S3. Hu, Q.; Nielsen, M. H.; Freeman, C. L.; Hamm, L. M.; Tao, J.; Lee, J. R. I.; Han, T. Y. J.; Becker, U.; Harding, J. H.; Dove, P. M.; De Yoreo, J. J., *Faraday Discuss*, 2012, **159**, 509-523.

S4. Owens, D.K., Wendt, R.C., *J. Appl. Polym. Sci.*, 1969, **13**, 1741-1747.

S5. Konda, A.; Taylor, J. M.; Stoller, M. A.; Morin, S. A., *Lab Chip*, 2015, **9** 2009-2017.

S6. Abdullah, A. M.; Li, X. L.; Braun, P. V.; Rogers, J. A.; Hsia, K. J., *Adv. Mater.*, 2018, **30**, 1801669.